Geobiology (2008), 6, 21–32 DOI: 10.1111/j.1472-4669.2007.00133.x

Wave and sediment dynamics along a shallow subtidal sandy beach inhabited by modern stromatolites

J. E. ECKMAN,[1] M. S. ANDRES,[2,*] R. L. MARINELLI,[3,†] E. BOWLIN,[2] R. P. REID,[2] R. J. ASPDEN[4] AND D. M. PATERSON[4]

[1]*Office of Naval Research, Code 32, 875 N. Randolph St., Arlington, VA 22203-1995, USA*
[2]*Marine Geology and Geophysics, Rosenstiel School of Marine and Atmospheric Sciences, University of Miami, 4600 Rickenbacker Causeway, Miami, FL 33149-1098, USA*
[3]*Chesapeake Biological Laboratory, Center for Environmental and Estuarine Sciences, University of Maryland, 1 Williams Street, PO Box 38, Solomons, MD 20688, USA*
[4]*School of Biology, Gatty Marine Research Institute, University of St Andrews, St Andrews, Fife KY16 8LB, UK*

ABSTRACT

To help define the habitat of modern marine stromatolites, wave-dominated flow and sediment transport were studied in the shallow subtidal region (1–2 m depth) along the slightly concave, windward face of Highborne Cay, Exuma, Bahamas – the only face of the cay that includes a population of stromatolites concentrated near the region of highest curvature of the beach. Wave energy impacting this island's most exposed beach was driven by local wind forcing which increases largely in response to the passage of atmospheric disturbances that typically affect the region for periods of a few days. Although some wave energy is almost always noted (maximum horizontal orbital speeds at the bottom are rarely <10 cm s^{-1}), wave conditions remain comparatively calm until local winds increase above speeds of ≈3–4 m s^{-1} at which point maximum wave speeds rapidly increase to 50–80 cm s^{-1}. Stromatolites, which are largely restricted to the shoreward side of a shallow platform reef, are sheltered by the reef beyond which wave speeds are one to four times higher (depending on tidal stage). Moreover, stromatolite populations are predominantly found along a region of this wave-exposed beach that experiences comparatively reduced wave energy because of the curved morphology of the island's face. Maximum wave speeds are 1.4 to 2 times higher along more northern sections of the beach just beyond the locus of stromatolite populations. A quantitative model of sediment transport was developed that accurately predicted accumulation of suspended sediment in sediment traps deployed in the shallow subtidal zone along this beach. This model, coupled with *in situ* wave records, indicates that gross rates of suspended sediment deposition should be two to three times higher northward of the main stromatolite populations. Regions of the beach containing stromatolites nevertheless should experience significant rates of gross suspended sediment deposition averaging 7–10 g cm^{-2} day^{-1} (≈4–6 cm day^{-1}). Results suggest that one axis of the habitat of modern marine stromatolites may be defined by a comparatively narrow range of flow energy and sediment transport conditions.

Received 05 January 2007; accepted 02 October 2007

Corresponding author: J. E. Eckman. Tel.: (703)-696-4590; fax: (703)-696-2007; e-mail: jim.eckman@navy.mil

INTRODUCTION

Stromatolites are a robust and long-lasting form of laminated microbial mat (Paerl *et al.*, 1993) that provide the earliest macroscopic evidence of life in the fossil record (Schopf, 1996). The microorganisms responsible for ancient stromatolites, which were a dominant life form on Earth for more than 2 billion years, may also have been critical to the generation of atmospheric oxygen (Des Marais, 1991; Knoll, 1992). Stromatolites declined abruptly in the fossil record with the evolution of multicellular life (Grotzinger, 1990; Knoll, 1992; Grotzinger & Knoll, 1999), presumably because of the superior competitive abilities of metazoa regarding overgrowth and colonization. Marine stromatolites persist in the modern world, but their distribution

*Present address: Chevron Energy Technology Company, 6001 Bollinger Canyon Road, D-1184, San Ramon, CA 94583-2324, USA
†Present address: Antarctic Biology and Medicine, Office of Polar Programs, National Science Foundation, 4201 Wilson Blvd., Arlington, VA 22203, USA

is highly restricted. Known locations include a hypersaline environment in Shark Bay, Australia (Logan, 1961; Davis, 1970; Hoffman, 1976), and several shallow subtidal regions along the margins of Exuma Sound in the Bahamas (Dravis, 1983; Dill *et al.*, 1986; Reid *et al.*, 1995; MacIntyre *et al.*, 1996).

It is believed that habitats capable of sustaining modern marine stromatolites in open-ocean conditions require at least episodic periods of intense fluid and sediment transport, including periods of sustained burial (e.g. Dravis, 1983; Dill *et al.*, 1986; Reid *et al.*, 1999; Andres & Reid, 2006). Such conditions apparently are required to prevent overgrowth and destruction of the mat by epilithic algae or grazing/burrowing invertebrates (Dill *et al.*, 1986; MacIntyre *et al.*, 1996; Andres & Reid, 2006). These concepts are well argued but are based largely on qualitative observation (for an exception see Steneck *et al.*, 1999). Quantitative information is desperately needed to help evaluate this theory and to accurately describe the physical habitat of modern marine stromatolites. Such data may prove useful in interpreting environmental conditions inferred from the fossil record.

With that need in mind we report here on key results from a multiyear investigation of the physics and sediment dynamics of a shallow subtidal environment located off the eastward (windward) facing beach of an island in the Bahamas that contains a large population of living marine stromatolites (Reid *et al.*, 1999; Andres & Reid, 2006). Our study considers not only the flow and sediment dynamic properties of the stromatolite habitat, but also the properties of adjoining regions along the beach that contain possibly stressed stromatolitic mats (i.e. mats greatly reduced in size or relief), and locales where stromatolites are absent. As such, our results provide an unprecedented depiction of the physical conditions pertinent to growth and survival of these mats, and help to constrain the physical axis of inhabitable space of this life form.

STUDY SITE

Stromatolites are found in the shallow subtidal zone along the 3-km-long, eastward-facing (windward) beach of Highborne Cay, Exuma, Bahamas (24°43′N, 76°49′W) (Fig. 1). They are not found along other faces of the island that are more protected from winds and waves. The beach system is and has been minimally impacted by human influence due to the extremely low population of the island, and is described by Andres & Reid (2006). To briefly review, a dominant feature of the shallow subtidal region (1–2 m depth) along a portion of this beach is a calcareous platform reef of variable width (visible in Fig. 1B,C). The surface of the shallow reef, which typically extends only ≈10–30 cm above sand level, is dominated on the seaward side by branching coralline algae (*Neogoniolithon strictum*) and by living stromatolites on the shoreward platform. The platform reef is widest (20–50 m) near the most concave portion of the island's eastern face (Sites 1–2 in Fig. 1C). The reef decreases in width (typically <10 m) toward the north and is restricted to more shoreward locations at Sites 3–5. The reef becomes discontinuous further northward at Sites 7–8. By Site 9 (≈675 m north of Site 1) reefs become discrete within a shallow subtidal region dominated by open sand. North of Site 10 (≈875 m north of Site 1) exposed stromatolite reefs are rare, small and isolated.

Sediments in the swash zone and shallow subtidal are ooid sands with a median grain size of 175–275 μm at Sites 1–10, but coarsen significantly to the north (see below and Reid *et al.*, 1999). Tides at Highborne Cay are semidiurnal with a maximum range of ≈1 m. Stromatolites are typically immersed except for rare periods of exposure during the lowest tides, and even then are bathed by breaking waves. Based on U/Th dating of authigenically precipitated carbonate in laminae it appears that stromatolites have been present along this beach in the shallow subtidal for up to 900 years and dominant in the back reef for the last 500 years (Andres *et al.*, in press).

METHODS

Wind patterns

Wind speed and direction were measured using a permanent weather station mounted on the East-facing beach a few meters above the high tide level near Site 6. This location provides an accurate record of the dominant easterly winds. Wind speed and direction were recorded every 15 min. A long-term record of winds, occasionally punctuated due to maintenance needs or storm damage, is available starting in November 2003 and continuing at least into summer of 2006.

Wave dynamics

The spatial and temporal properties of wave-driven flow that dominates the shallow subtidal zone were studied using a combination of wave gauges and an acoustic-Doppler velocimeter. Two Dobie Wave Gauges (NIWA Instrument Systems, Christchurch, New Zealand) were used as our principal instruments for measuring wave dynamics over a 3-year period beginning in June 2003. This gauge is primarily a fast-response pressure sensor driven by an internal, programmable microcomputer. Wave properties (e.g. mean period, significant wave height [mean height of the highest one-third of waves], wave length) and important characteristics of the wave-driven flow (e.g. maximum horizontal orbital flow speed at the bed for waves of the significant height – hereafter called the *maximum wave speed* for brevity) are calculated from high-frequency pressure records using linear wave theory. The accuracy of these calculations was assessed by comparing them to direct measurements of flow (see below).

Our strategy was to deploy both instruments synchronously on weighted frames on the bottom at approximately equivalent depths (the region inhabited by stromatolites, ≈1 m below low water). Instrument positions were mapped by taking a

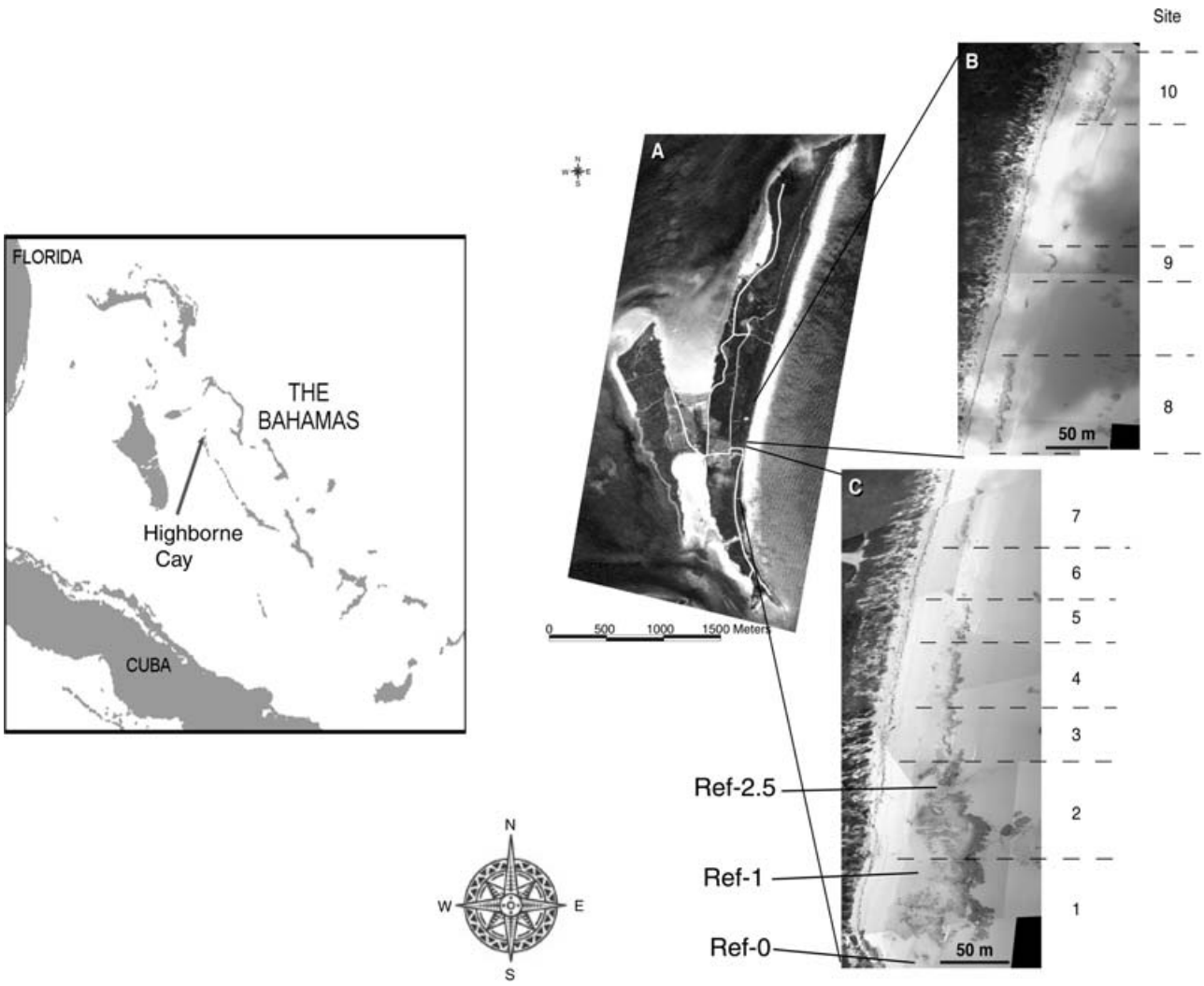

Fig. 1 Map of Bahamas and photograph of Highborne Cay (A), showing locations of Sites 1–10 (photographs B, C) along the eastward (windward) facing beach. Locations of three Reference Sites (Ref-0, -1 and -2.5) are indicated.

reading over the instruments *in situ* with a hand-held GPS (accurate to within ≈3 m). Each gauge was programmed to record a 1024-point burst at 5 Hz (3.41 min record) every 15 min. The two meters were programmed to turn on and off synchronously to enable direct comparisons to be made of the wave energy at two locations along the beach. Wave measurements were corrected for depth (i.e. standardized to a reference site's depth) using linear wave theory. We selected two sites to serve as reference sites (one replaced the other when episodic sand waves temporarily buried a site, and the two reference sites were intensively cross-calibrated). One reference site (Ref-1 in Fig. 1) was located just shoreward of a large stromatolite head at Site 1 (24°42.736′N: 76°49.173′W), and the other (Ref-2.5 in Fig. 1) was 103 m to the north, in a sandy cut open to the offshore (24°42.791′N: 76°49.162′W) between stromatolite heads at Sites 2 and 3. Whenever wave gauges were deployed, one gauge was placed at one of the reference sites (the fixed gauge), while the other was placed at another locale (the moveable gauge). The moveable gauge was left in place for a period of days to weeks, after which it was moved to another position along the beach. This strategy was used while placing the moveable gauge at dozens of locations along the entire length of the east-facing beach. By this means we are able to compare wave energy at any location along the beach to wave energy experienced simultaneously at a reference site, thus enabling us to use the series of comparatively short-term measurements to establish a high spatial resolution map of relative wave energy along the entire beach. The validity of this assumption was evaluated, in part, by comparisons with gross spatial patterns of sediment grain size distribution along the beach, which provide a more time-integrated measure of differences in energy along the beach.

Wave gauge data were complemented with some direct measurements of wave-dominated current velocity and suspended

sediment concentrations. These data were useful for checking the accuracy of flow calculations made from pressure records. Current velocity was measured using a SonTek (San Diego, CA, USA) Ocean Probe Model ADVocean Acoustic Doppler Velocimeter (ADV) recording 3-D vectors of flow at 10 Hz. This instrument records velocity within a volume of ≈2 cm^3. The ADV head was positioned such that high frequency records of wave velocity were collected within a few centimeters of the bottom, outside of the very thin wave boundary layer and at a height where the horizontal orbital flow created by waves would be maximal. From 13 to 17 November 2003, the ADV was used in conjunction with a wave gauge placed ≈1 m away. Data were collected in a series of 3- to 5-min bursts every 20 min over periods of 4–8 h each day at five sites distributed along the beach (within Sites 1, 2, 3, 10 and at the boundary between Sites 7 and 8) in water averaging ≈0.7-m depth. The ADV also was equipped with an optical backscatter sensor (OBS) (model OBS-3; D & A Instruments, Logan, UT, USA) that is capable of measuring concentrations of suspended sediment. The OBS was calibrated just prior to deployment using suspensions of sand collected from the low intertidal zone at Highborne beach. The calibration was linear and strong ($r^2 = 0.98$) in the range of 0–10 g l^{-1}. In the field the OBS sensor recorded suspended sediment concentrations at a height of a few centimeters above bottom that varied slightly among deployments.

Sediment transport

Two techniques were used to relate wave measurements to gross sediment transport and deposition. First, we compared directly measured (ADV) and calculated (wave gauge) maximum wave speeds to measurements collected using the OBS (above). The second technique involved empirical measurements of sediment resuspension and deposition. Triplicate sediment traps were deployed ≈1 m from a wave gauge on 13 occasions in July 2004. Deployments were at various locations all south of Site 10. A trap was a vertical tube 29 cm long and 2.8 cm in diameter that was capped at the bottom and secured to a stake anchored into the sediments (Todd *et al.*, 2006). Each trap was fitted with internal baffles to prevent loss of captured material. A trap was positioned such that its opening was 30 cm above the bottom. Thus, only suspended sediments were captured during their downward fall after suspension by waves. Triplicate traps were deployed for 24 h at which time they were all capped, collected, and returned to the laboratory, and the contents dried, weighed and sorted for grain size. Rates of collection of suspended sands were related to time-integrated measurements of wave velocity and bottom stress using theories for wave boundary layers (e.g. Grant & Madsen, 1982; Middleton & Southard, 1984) and sediment transport (e.g. Miller *et al.*, 1977), as follows.

Sediment transport theory shows that

$$q \propto (\tau - \tau_{crit})^{\beta} \quad (1)$$

where q is the horizontal sediment transport rate, τ is the bed shear stress, τ_{crit} is the critical erosion stress and $\beta \approx 1.5$ (Jumars & Nowell, 1984). The stress (τ) is often expressed in terms of a friction velocity (u^*), where $u^* = (\tau/\rho)^{1/2}$ and ρ is seawater density. Both stress terms can be calculated.

Grant & Madsen (1982) show that u^*_{wave} relates to the maximum horizontal wave velocity near the seafloor (u_b) as

$$u_{*wave} = u_b \sqrt{(f_w/2)} \quad (2)$$

where f_w is a wave friction factor. For beds of any appreciable roughness $f_w \approx 0.24$. Therefore

$$\tau = \rho u_{*wave}{}^2 = 1.025(0.346u_b)^2 = 0.12u_b^2 \quad (3)$$

Eq. (3) allows estimation of the bed stress from values of maximum wave speed obtained from the wave gauges. Provisionally, we use the maximum wave speed as an approximation of u_b.

Sediment trap openings were 30 cm above bed level (≈30% of flow depth) and it is necessary to define a τ_{crit} at which sediments would have been suspended to this height. Figures 6–22 in Middleton & Southard (1984) indicates that this condition requires

$$w/\kappa u^* < 2, \text{ or } w/u^* < 0.8 \quad (4)$$

where w is the settling velocity of the sediment grains and κ is van Karman's constant (≈0.4). Therefore for suspended material to fall into traps

$$u_{*crit} = 1.25 \text{ w, or } \tau_{crit} = \rho(1.25w)^2 = 1.6w^2 \quad (5)$$

The settling velocity of a calcite particle ($\rho_s = 2.71$ g cm^{-3}) of median grain size (D) of Highborne beach sand can be estimated by empirical relationships presented in Hallermeier (1981).

The above relationships allow Eq. (1) to be evaluated. To predict the total horizontal transport of suspended sediments the time-dependent transport rate expressed in Eq. (1) is integrated over the time of trap deployment (t). This time-integrated transport should scale monotonically to the amount of material (M) that accumulated in traps (the gross vertical deposition of suspended sediments)

$$M \propto \int_0^t q \partial t \quad (6)$$

Rates of collection of suspended sands in traps were compared to the integrated transport defined in Eq. (6).

RESULTS

Wave gauge and ADV comparisons

Pressure records collected by the wave gauge are analysed using linear wave theory to estimate the maximum wave speed.

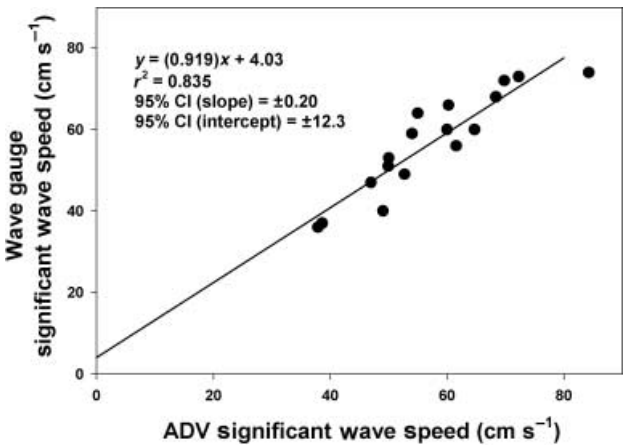

Fig. 2 Comparison of significant wave speed calculated from high-frequency pressure records to that measured directly and simultaneously using an ADV located ≈1 m away. Data points were obtained between 13 and 17 November 2003 among five sites distributed along the beach (within Sites 1, 2, 3, and 10 and at the boundary between Sites 7 and 8). CI – statistical confidence interval of slope or intercept.

Especially given the shallow flow depths in the region studied here it is important to evaluate the validity of this calculation. ADV records of horizontal flow speed collected at five locations along the beach simultaneously with wave records were examined, and the maximum wave speeds obtained from each instrument were intercompared. As illustrated in Fig. 2, the match between direct measurements of maximum wave speed and the speed calculated from pressure records was very good ($r^2 = 0.835$), despite the ≈1-m separation of the two instruments at all sites. The confidence intervals (CI) of the slope and intercept of the regression line relating the two sets of measurements include 1.0 and 0 cm s^{-1}, respectively, which is expected if both instruments accurately measured or calculated the same parameter. Therefore, it is reasonable to conclude that wave speed calculations by the wave gauges generally are accurate in this shallow subtidal environment.

Wind and wave patterns

To provide an example of the time series of wave patterns recorded, a 106-day record (14 November 2005 to 28 February 2006) of maximum wave speed at Reference Site 2.5 is illustrated in Fig. 3A. The nearshore region on this windward beach is never totally still (maximum wave speeds of at least a few centimeters per second are always noted). Periods of comparative calm are punctuated by frequent periods of elevated wave activity during which maximum wave speeds increase to 40–60 cm s^{-1} and remain elevated for periods of several days typically. Maximum wave speeds only occasionally exceed 70 cm s^{-1} though short-lived surges to 80–100 cm s^{-1} occur rarely.

A more detailed examination of a subset of these data (22 November to 11 December 2005), plus concurrent wind records, is illustrated in Fig. 3B. This plot clearly indicates that nearshore wave dynamics are tightly linked to local wind conditions. Wave conditions remain comparatively calm until local winds at beach level increase above speeds of ≈3 m s^{-1}. Winds exceeding this speed occur primarily in response to the passage of atmospheric disturbances that typically affect the region for periods of a few days before winds calm. Maximum wave speeds increase rapidly in response to increasing local winds, and wave energy declines rapidly once winds decrease below 3 m s^{-1}. Figure 3B also indicates that there is a tidal periodicity in the maximum wave speed. This periodicity in the impact of waves on the bottom is expected given the relatively large change in water depth (near doubling) over the semidiurnal tidal cycle in the shallow waters inhabited by stromatolites.

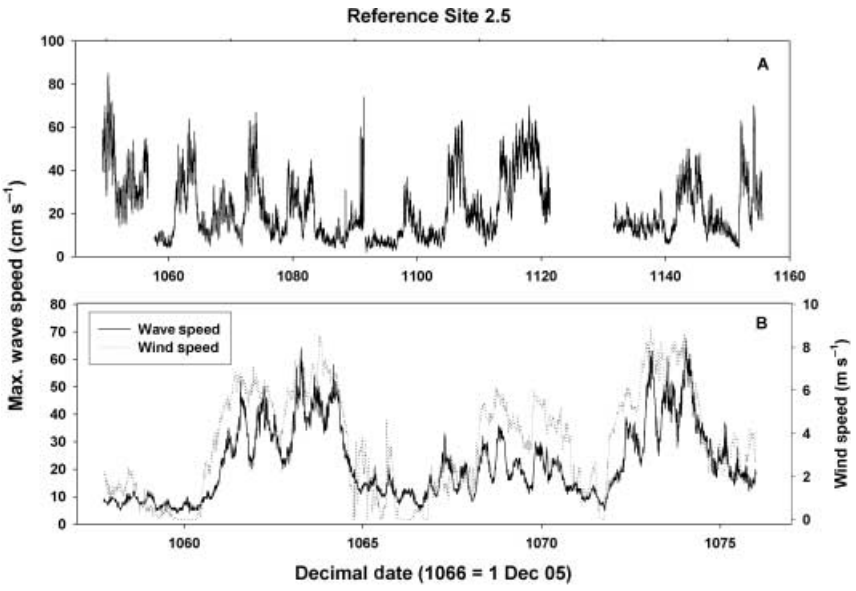

Fig. 3 (A) A 106-day record of maximum wave speed at Reference Site 2.5 between November 2005 and February 2006. (B) A shorter-term (41 days) record of wave and local wind speed extracted from A illustrating tight coupling of local wind and maximum wave speeds.

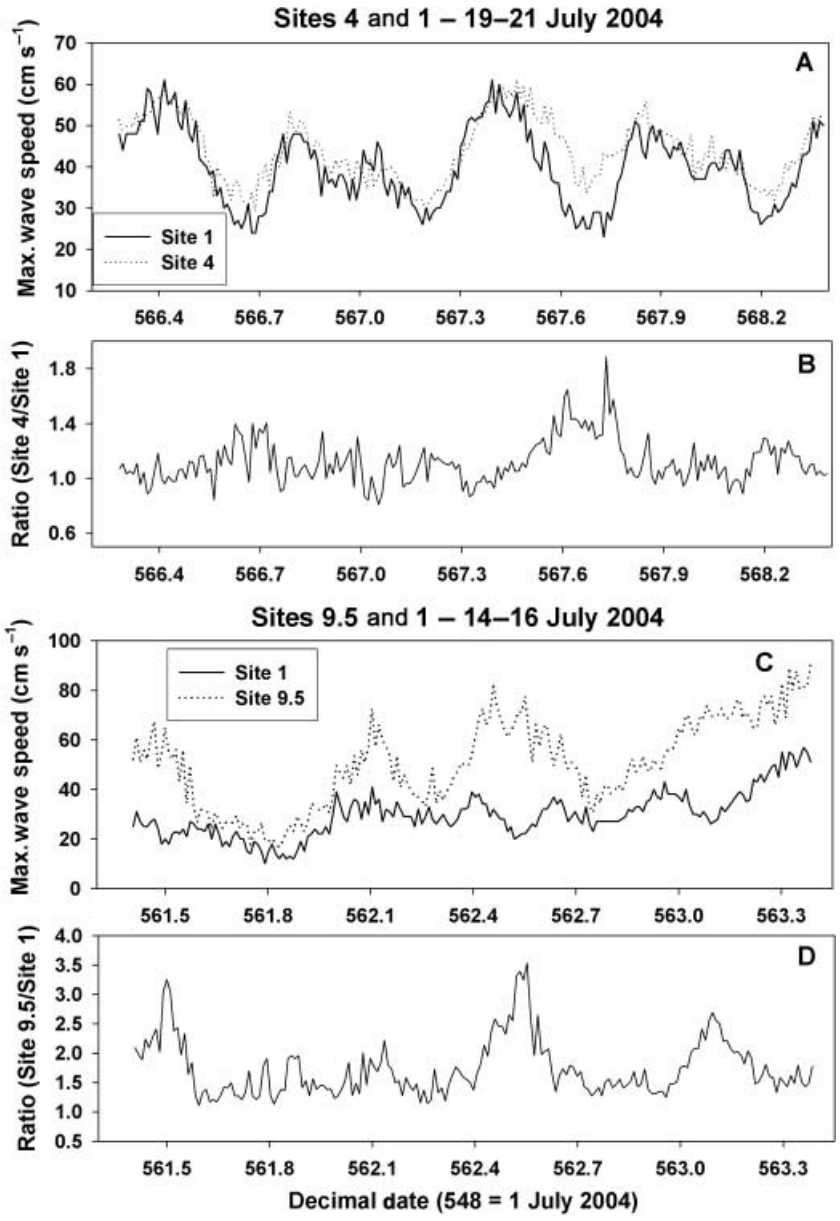

Fig. 4 Short-term records comparing maximum wave speeds at two locations along the beach. (A) Maximum wave speeds at Sites 4 and 1 on 19–21 July 2004. (B) Ratio of two speeds. (C) Maximum wave speeds at Site 9.5 and 1 on 14–16 July 2004. (D) Ratio of two speeds.

Spatial patterns in wave dynamics

To illustrate both similarities and differences noted among sites in wave exposure, Fig. 4 illustrates short-term (2 days) comparisons of wave energy at two sites, relative to Reference Site 1. As at Site 1 the wave gauge placed at Site 4 (19–21 July 2004) was located just inside the reef; the two sites are separated by 200 m. Maximum wave speeds were very similar at the two sites and identically tracked the semidiurnal tide (Fig. 4A). The ratio of maximum wave speeds at the two sites remained very close to unity (Fig. 4B), and averaged 1.12 times higher at Site 4, indicating that the two sites experienced essentially identical wave energy. In contrast, wave dynamics at Site 9.5 (a sandy beach between Sites 9 and 10, unprotected by a fringing reef – Fig. 1B) were notably different from that at the reference Site 1, which is located 785 m to the south. Maximum wave speeds at Site 9.5 were consistently higher than those at Site 1 (14–16 July 2004) and the two sites did not closely track each other (Fig. 4C). Wave speeds at Site 9.5 at times were three times higher than at Site 1 and averaged 1.7 times higher over the 2-day period (Fig. 4D).

Comparisons such as these were repeated along the entire length of the beach to produce a plot of relative wave energy (i.e. standardized to reference Site 1) illustrated in Fig. 5. There are two major patterns evident in this graph. First, southward of Site 9.5 (distances <750 m from Site 0, position shown in Fig. 1C) the wave energy remains relatively constant, with maximum wave speeds within ±30% of those recorded at

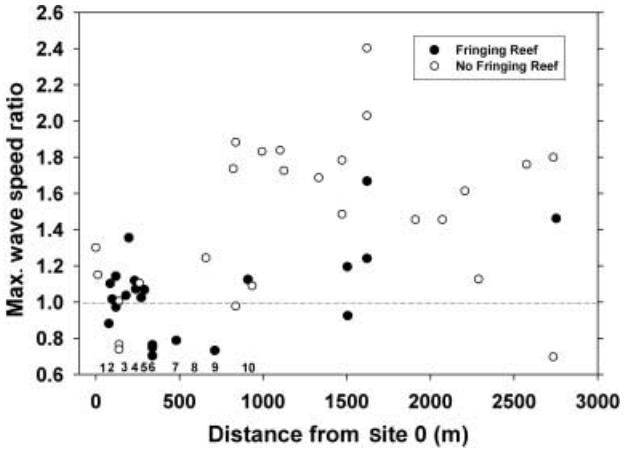

Fig. 5 Maximum wave speed relative to that predicted simultaneously for Reference Site 1 as a function of distance along the beach (distance = 0 at Reference Site 0 (Ref-0 in Fig. 1)). Positions of Sites 1–10 are noted along the abscissa. Ratios are distinguished based on presence (closed circles) or absence (open circles) of a seaward fringing reef at each location of measurement. Positions of Sites 1–10 are noted along the abscissa.

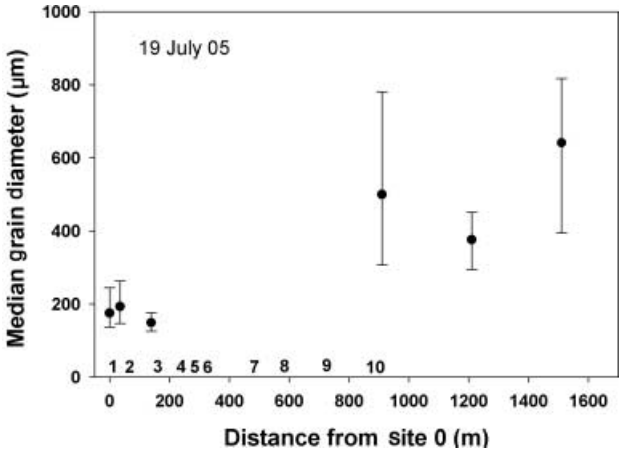

Fig. 6 Median sediment grain diameter as a function of distance along the beach (distance = 0 at Reference Site 0 (Ref-0 in Fig. 1)). 'Confidence limits' of points illustrate lower and upper quartiles (25th and 75th percentiles) of grain diameter. Positions of Sites 1–10 are noted along the abscissa.

reference Site 1 (dashed line in Fig. 5). There was no obvious gradient alongshore within this portion of the beach. However, this portion of beach, which contains the large stromatolite populations inside the platform reef, clearly differs from more northern reaches of the beach. An abrupt increase in wave energy occurs north of Site 9 at distances > 750 m from Site 0. Although considerable variability is noted there is an obvious pattern of maximum wave speeds 1.3 to 2.4 times higher than are observed to the south. Second, this pattern appears only slightly modified by the presence or absence of the platform reef. Sites that are open to the ocean (open circles in Fig. 5) exhibit this pattern somewhat more clearly than sites characterized by the presence of a seaward fringing reef (closed circles). Simple Student *t*-tests confirm these statements. For sites open to the ocean maximum wave speeds north of Site 9 were significantly higher (an average of 1.52 times) than wave speeds at open sites southward of Site 9 ($P < 0.0009$). When a seaward platform reef was present maximum wave speeds sites north of Site 9 were significantly higher (an average of 1.32 times) than speeds at protected sites southward of Site 9 ($P < 0.002$).

The applicability of this pattern to timescales longer than the duration of short-term wave records is confirmed by examining the pattern of sediment grain size along the beach. The median grain size of sediments collected in the low intertidal zone on 19 July 2005 shows a substantial and abrupt coarsening of sediments north of Site 10 (Fig. 6), a pattern that mimics that illustrated in Fig. 5. This parameter reflects a more time-integrated response to wave energy and similarly indicates a more energetic beach north of the main population of stromatolites.

Despite the general similarity of average wave energy throughout the shallow subtidal zone south of Site 10, it is clear that the presence of a fringing reef affords some additional protection from wave energy to the back-reef zone inhabited by stromatolites. As an example, Fig. 7 illustrates a 6-day record (17–23 June 2006) of wave speeds recorded in the fore-reef and back-reef zones at reference Site 1, where the fringing reef is widest (≈50 m). During the more energetic first half of the record (decimal dates 1264.5–1267.5) maximum wave speeds were highest at low tide in the fore-reef zone at the same time they were reaching minima in the back-reef region (Fig. 7A). Therefore, at low tide, the back reef was experiencing the greatest protection from waves by the fringing reef. At high tide, however, wave speeds were comparable at both fore- and back-reef zones. Thus, there is a decidedly tidal pattern in the ratio (fore/back) of wave speeds (Fig. 7B), which varied from ≈1.0 at high tide to 3–4 at low tide.

Waves and sediment transport

Our measurements allow us to directly compare the interactions between wave energy and sediment transport across a range of spatio-temporal scales. These scales range from high-frequency, nearly point measurements of flow speed and suspended sediment concentration (obtained from the OBS sensor) to time integrated (multiday) measurements of gross sediment deposition (measured via sediment traps) compared among sites separated by 100s of meters. Simultaneous records of wave speed and suspended sediment concentrations surprisingly reveal a general discordance between the two theoretically connected phenomena, at least at high frequencies. As illustrated in Fig. 8 bursts in concentrations of suspended sediment may occasionally follow bursts in flow speed with a lag of perhaps a few tenths of a second, but most bursts in flow speed are not associated with any concordant change in sediment suspension.

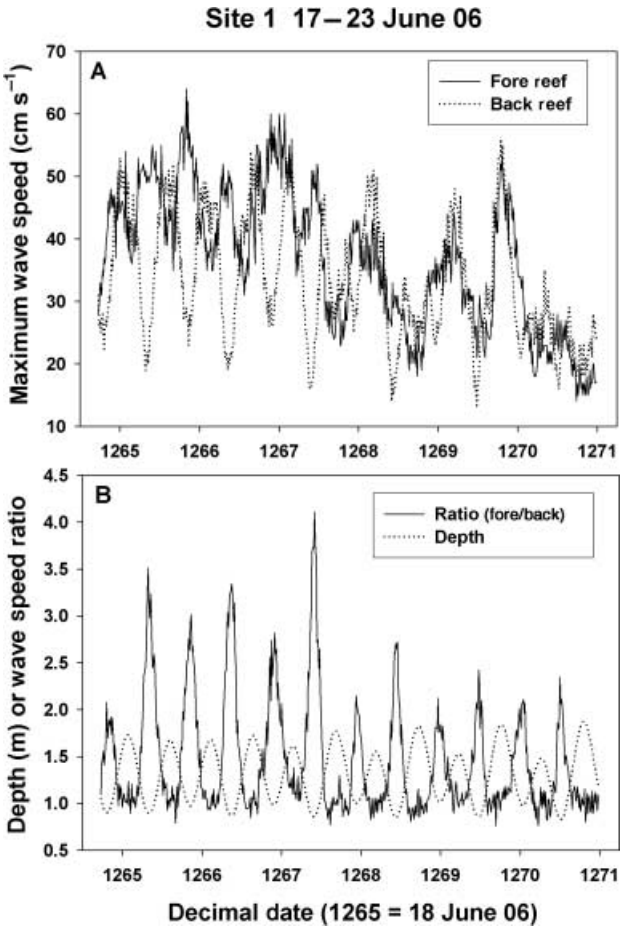

Fig. 7 (A) Maximum wave speeds calculated seaward (Fore Reef) and landward (Back Reef) of the fringing platform reef at Reference Site 1 between 17 and 23 June 2006. (B) Ratio of wave speeds relative to tidal stage (depth).

This highly localized, higher-frequency discordance does not suggest that sediment transport is decoupled from the intensity of wave energy over larger spatio-temporal scales, however. This is evident from our sediment trap studies that integrate over timescales of approximately 1 day. As illustrated in Fig. 9 there is good agreement between the amount of material captured by sediment traps in 24 h, and that predicted by theory ($r^2 = 0.70$). Because the intercept of the relationship illustrated in Fig. 9 is not significantly different from zero (i.e. zero transport is measured when zero is predicted), it can be concluded that our method of estimating the stress and the critical stress of suspended sediments is reasonable. Figure 9 also indicates that we can use wave gauge data to calculate the gross vertical flux of suspended material along Highborne Cay beach.

The result of such an exercise is illustrated in Fig. 10 for two paired time series of wave data that contrast conditions at northern (higher energy) vs. southern (lower energy) portions of the beach. Between 27 June and 10 July 2006 maximum wave speeds and predicted rates of sediment accumulation were generally lower at reference Site 1 than at Site 11C, located 1600 m to the north (Fig. 10A–C). The difference was most pronounced during the 3-day period from 1 to 3 July (decimal dates 1278–1280) and a 2-day period from 9 to 10 July (decimal dates 1286–1287), during which times wind speeds of >4 m s^{-1} were sustained. The impact of increased winds on local wave intensity and sediment transport was most obvious at the exposed, northern-most site. This pattern is predicted to have produced a time-integrated amount of gross sediment deposition at Site 11C (386 g cm^{-2}, or 33.3 g cm^{-2} day^{-1} on average) that was more than three times that predicted at Reference Site 1 (116 g cm^{-2}, or 10.1 g cm^{-2} day^{-1} on average) (Fig. 10C), despite the increased grain size (and higher erosion threshold) of sediments at Site 11C. A similar pattern was noted between Site 11 C and Site 3 (1420 m to the south) between 13 July and 9 August 2006. Wave intensities and gross rates of sediment deposition were generally higher at the northern-most site on the beach (Fig. 10D–F). The differences between the sites were most noticeable during periods of high winds on 13–14 July and 27–29 July The gross deposition of sediment over this 27-day period was predicted to be 438 g cm^{-2} at Site 11C (18.7 g cm^{-2} day^{-1} on average), which is more than two times that predicted at the more southern Site 3 (198 g cm^{-2}, or 7.4 g cm^{-2} day^{-1} on average) (Fig. 10F).

DISCUSSION

Our results indicate that wave gauges, which are comparatively inexpensive, computer-controlled pressure sensors, can be used to accurately predict speeds of wave-driven flows even in very shallow water. It is clear that data obtained from these sensors, coupled with sediment transport theory, can be used to predict both spatial and temporal variability in vertical fluxes of suspended sediments with reasonable accuracy. Equipped with these tools we were able to demonstrate that modern marine stromatolites, which are found only along the windward and most wave exposed face of Highborne Cay, are focused in a shallow subtidal region of the beach that experiences the least wave energy along this face of the island. Almost certainly because of the curved morphology of the windward face of the island (which would tend to refract waves away from the beach's centre) maximum wave speeds are 1.4 to 2 times higher along more northern sections of the beach just beyond the locus of stromatolite populations. Moreover, within this central region of the beach stromatolites are largely restricted to the shoreward side of a platform reef that further shelters the mats from wave energy – on the seaward side of the reef wave speeds are one to four times higher (depending on tidal stage).

Although these data point to stromatolites inhabiting the least energetic portion of the windward (exposed) beach on Highborne Cay it would be incorrect to conclude that these unique microbial mats are not tolerant of flow and wave energy. In fact, the opposite is true as evidenced by the absence

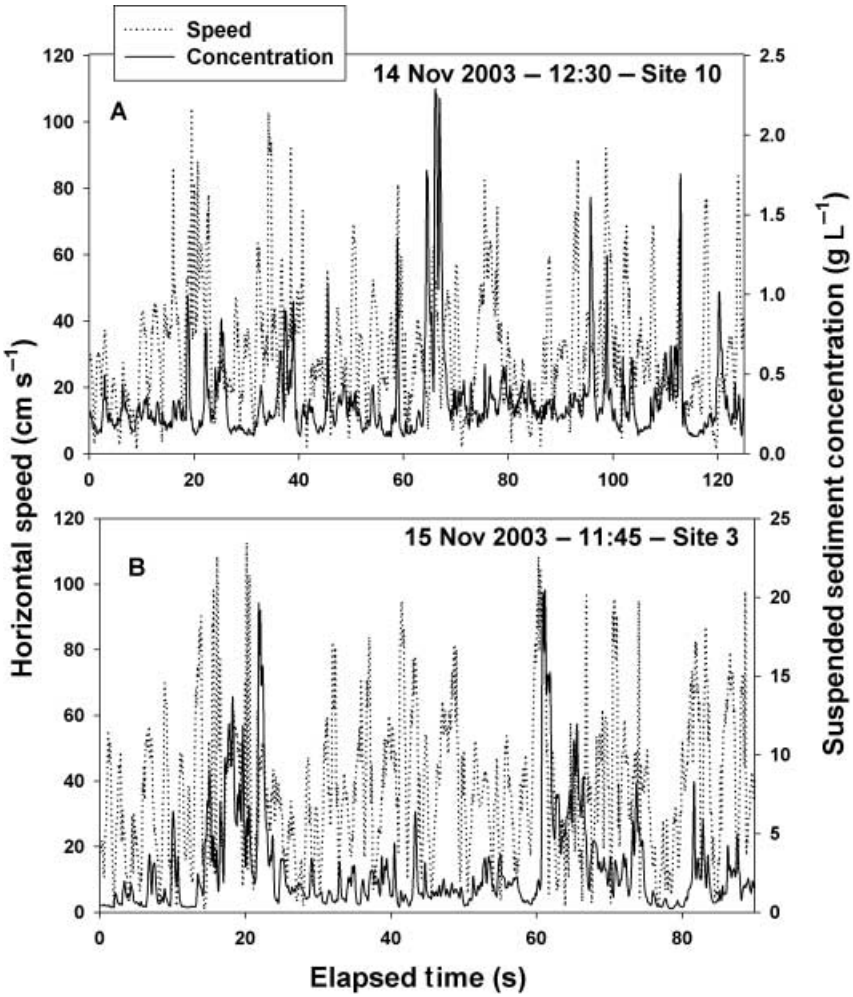

Fig. 8 Representative portions of high-frequency (10 Hz) measurements of horizontal speed measured using the ADV and suspended sediment concentration measured using the optical backscatter sensor collected at two sites in November 2003.

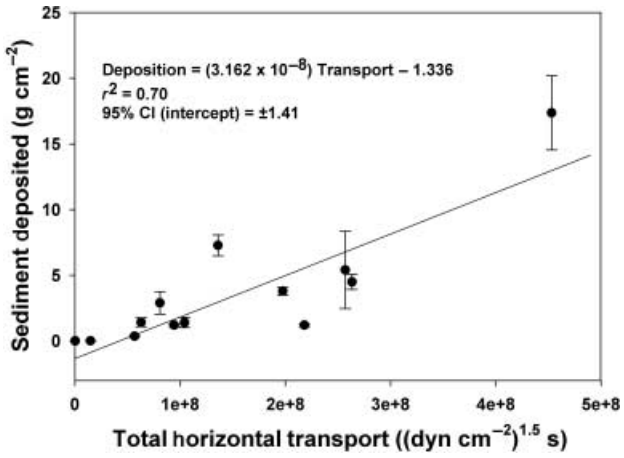

Fig. 9 Sediment accumulated in traps as a function of the total (time-integrated) horizontal transport predicted for the period of trap deployment at the location of each measurement. CI – statistical confidence interval of intercept.

of stromatolites along less-exposed faces of the island. Modern stromatolites are a form of microbial mat noteworthy for their requirement for comparatively high physical energy in terms of fluid and sediment transport (e.g. Dravis, 1983; Dill *et al.*, 1986; Reid *et al.*, 1999). In contrast, other forms of microbial mat typically require more benign conditions in terms of physical energy to persist (e.g. Cohen & Rosenberg, 1989; Noffke *et al.*, 2002).

The accepted explanation for the requirement for comparatively high flow energy by modern marine stromatolites is that frequent sediment transport, including periods of sustained burial, is required to prevent overgrowth and destruction of the mat by epilithic algae or grazing/burrowing invertebrates (Dill *et al.*, 1986; Macintryre *et al.*, 1986; Andres & Reid, 2006). Our field and model results suggest that stromatolites in the shallow subtidal region of Highborne Cay beach (i.e. south of Site 10) regularly experience gross rates of deposition of suspended sediments averaging 7–10 g cm^{-2} day^{-1} (Fig. 10) (or a vertical rate of deposition of ≈4–6 cm day^{-1} assuming a reasonable porosity for loosely packed calcareous sands), with

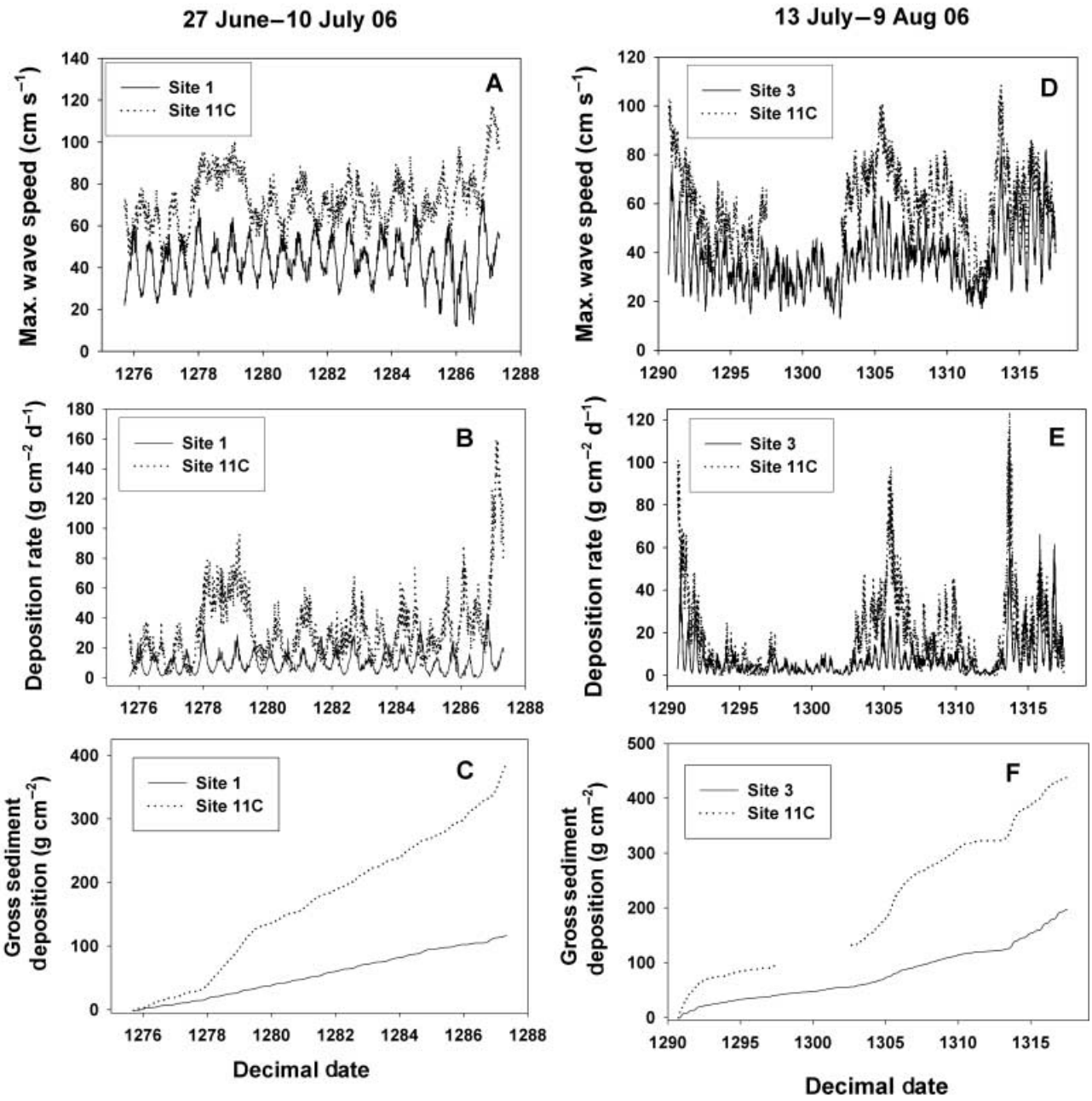

Fig. 10 Maximum wave speeds (A, D), instantaneous sediment deposition rates (B, E) and time-integrated amounts of gross sediment deposition (C, F) predicted at northern (Site 11C) and more southern (Sites 1 or 3) portions of the beach for two representative time blocks in summer of 2006. To obtain predictions illustrated in F, an average deposition rate for the previous few days was assumed for the 5-day break in the wave record at Site 11C in late July (decimal dates 1298–1302).

a daily range of ≈0.5–3 × that mean. It is interesting to note that this range of values is not greatly different from gross sedimentation rates measured by Steneck *et al.* (1999) in stromatolite reefs in a subtidal algal ridge system elsewhere (Stocking Island) in the Exuma Cays, Bahamas. They reported gross sedimentation rates averaging ≈24 g cm^{-2} day^{-1} (calculated from data reported in their Fig. 4), with an apparent range of ≈0.5–2 ×. The similarity in these two ranges, obtained >100 km and a decade apart, suggests the interesting possibility that the level of flow energy capable of producing these sediment fluxes may be that necessary to permit stromatolite growth in open marine environments while preventing destructive overgrowth.

What is equally interesting is the implication from our data and the observed distributions of stromatolites along Highborne Cay that their inhabitable range of flow energy and sediment flux might be comparatively narrow. As previously noted, stromatolites are not found along more wave-protected portions

of Highborne Cay, are located on the windward beach only on the protected, landward side of the shallow platform reef (where wave speeds are significantly reduced compared to the seaward edge – Fig. 7B), and are nearly absent along more northward sections of the beach, where there is some platform reef available for colonization (see Fig. 1 in Reid *et al.*, 1999), but where wave energy and gross suspended sediment fluxes are significantly higher (Figs 5 and 10).

The limited quantitative information available regarding the physical dynamics of modern stromatolite habitats (Steneck *et al.*, 1999, and this study) therefore suggests that these mats inhabit sedimentologically energetic environments, but possibly within narrow limits. It is certainly worth investigating this further, for example by studying in more detail the physics and sediment dynamics of other environments where modern stromatolites are found. Prime candidates for such studies would be the subtidal sandy channels off Lee Stocking Island, Bahamas, where tall columnar stromatolites are found in deep channels characterized by tidally driven bedload transport (e.g. Dill *et al.*, 1986), as well as the shallow subtidal regions around Eleuthera Bank, Bahamas, that contain populations of high-relief stromatolites (Dravis, 1983). Such studies would greatly expand our understanding of conditions required for, or capable of, sustaining growth of modern marine stromatolites.

It is not obvious to us why the upper limit of habitable wave energy and sediment deposition rates should be so close to that minimum apparently required for stromatolite persistence, but several explanations are possible. For example, under higher energy conditions more frequent or longer lasting burial by shifting sands might prevent survival of mats that at least episodically require photosynthesis by oxygenic phototrophs (Reid *et al.*, 2000; Visscher & Stolz, 2005). It is also possible that higher levels of sediment transport might result in abrasive disruption of exopolymer secretion necessary for early surface lithification (Decho *et al.*, 2005). These hypotheses are amenable to experimental evaluation via transplants along Highborne Cay beach, for example, and such studies might prove highly illuminating.

Finally, it is worth noting that the gross levels of suspended sediment deposition reported here, as well as in Steneck *et al.* (1999), are based on accumulations in slightly elevated sediment traps. These fluxes of suspended sediment, which are certainly important to stromatolite accretion, nevertheless underestimate the true levels of sediment flux to which some stromatolites associated with shallow platform reefs are exposed. Bed load transport is largely responsible for migration of nearshore sand waves and will occasionally bury and uncover some low-lying portions of platform reef at Highborne Cay.

ACKNOWLEDGEMENTS

We thank Dr Pieter Visscher and his associates for providing and maintaining the meteorological station. Assistance in the field with the ADV and wave gauges was provided by Steve Engstrom, George Waldbusser and Nick Jabro. Patricia Gaspar assisted with illustrations and geopositioning data. Lillian Custals assisted with processing and reporting of data from the meteorological station. This paper was supported by grant EAR-0221796 from the US National Science Foundation, and grants N00014-98-1-0260 and N00014-06-1-0301 from the US Office of Naval Research. RIBS Contribution No. 40.

REFERENCES

Andres MS, Reid RP (2006) Growth morphologies of modern marine stromatolites: a case study from Highborne Cay, Bahamas. *Sedimentary Geology* **185**, 319–328.

Andres MS, Reid RP, Bowlin E, Gaspar AP, Eisenhauer A (in press) Microbes versus metazoans as dominant reef builders: insights from modern marine environments in the Exuma Cays, Bahamas. In *Perspectives in Sedimentary Geology: A Tribute to the Career of Robert Nathan Ginsburg* (eds Swart PK, Eberli GP, McKenzie JA). International Association of Sedimentologists Special Publication 41, Blackwell Publishing, Oxford, UK.

Cohen Y, Rosenberg E (1989) *Microbial Mats: Physiological Ecology of Benthic Microbial Communities*. American Society of Microbiology Publications, Washington, DC.

Davis GR (1970) Algal laminate sediments, Gladstone embayment, Shark Bay, Western Australia. *American Association of Petroleum Geologists Memoirs* **13**, 85–168.

Decho AW, Visscher PT, Reid RP (2005) Production and cycling of natural microbial exopolymers (EPS) within a marine stromatolite. *Palaeogeography, Palaeoclimatology, Palaeoecology* **219**, 71–86.

Des Marais DJ (1991) Microbial mats, stromatolites and the rise of oxygen in the Precambrian atmosphere. *Palaeogeography, Palaeoclimatology, Palaeoecology* **97**, 93–96.

Dill RF, Shinn EA, Jones AT, Kelly K, Steinen RP (1986) Giant subtidal stromatolites forming in normal salinity waters. *Nature* **324**, 55–58.

Dravis JJ (1983) Hardened subtidal stromatolites, Bahamas. *Science* **219**, 385–386.

Grant WD, Madsen OS (1982) Movable bed roughness in unsteady oscillatory flow. *Journal of Geophysical Research* **87**, 469–481.

Grotzinger JP (1990) Geochemical model for Proterozoic stromatolite decline. *American Scientist* **290**, 80–103.

Grotzinger JP, Knoll AH (1999) Stromatolites in Precambrian carbonates: evolutionary mileposts or environmental dipsticks? *Annual Review of Earth and Planetary Science* **27**, 313–358.

Hallermeier RJ (1981) Terminal settling velocity of commonly occurring sand grains. *Sedimentology* **28**, 859–865.

Hoffman P (1976) Stromatolite morphogenesis in Shark Bay, Western Australia. In *Stromatolites* (ed. Walter M), pp. 261–273. Elsevier Science Publications, Amsterdam.

Jumars PA, Nowell ARM (1984) Effects of benthos on sediment transport: difficulties with functional grouping. *Continental Shelf Research* **3**, 115–130.

Knoll AH (1992) The early evolution of eukaryotes: a geological perspective. *Science* **256**, 622–627.

Logan BW (1961) Cryptozoan and associated stromatolites from the Recent, Shark Bay, Western Australia. *Journal of Geology* **69**, 517–533.

MacIntyre HL, Reid PR, Steneck RS (1996) Growth history of stromatolites in a Holocene fringing reef, Stocking Island, Bahamas. *Journal of Sedimentary Research* **66**, 231–242.

Middleton GV, Southard JB (1984) *Mechanics of Sediment Transport*, 2nd edn. Society of Economic Paleontologists and Mineralogists, Tulsa, Oklahoma.

Miller MC, McCave IN, Komar PD (1977) Threshold of sediment motion under unidirectional currents. *Sedimentology* **24**, 507–527.

Noffke N, Knoll AH, Grotzinger JP (2002) Sedimentary controls on the formation and preservation of microbial mats in siliciclastic deposits: a case study from the Upper Neoproterozoic Nama Group, Namibia. *Palaios* **17**, 533–544.

Paerl HW, Joye SB, Fitzpatrick M (1993) Evaluation of nutrient limitation of CO_2 and N_2 fixation in marine microbial mats. *Marine Ecology Progress Series* **101**, 297–306.

Reid RP, MacIntyre IG, Browne KM, Steneck RS, Miller T (1995) Modern marine stromatolites in the Exuma Cays, Bahamas: uncommonly common. *Facies* **33**, 1–18.

Reid RP, MacIntyre IG, Steneck RS (1999) A microbialite/algal ridge fringing reef complex, Highborne Cay, Bahamas. *Atoll Research Bulletin* **465**, 1–18.

Reid RP, Visscher PT, Decho AW *et al.* (2000) The role of microbes in accretion, lamination and early lithification of modern marine stromatolites. *Nature* **406**, 989–992.

Schopf JW (1996) Are the oldest fossils cyanobacteria? In *Evolution of Microbial Life* (eds Roberts DM, Sharp P, Alderson G, Collins MB), pp. 23–62. Cambridge University Press, Washington, DC.

Steneck RS, MacIntyre IG, Reid RP (1999) A unique algal ridge system in the Exuma Cays, Bahamas. *Coral Reefs* **16**, 29–37.

Todd CD, Phelan PJC, Weinmann BE *et al.* (2006) Improvements to a passive trap for quantifying barnacle larval supply to semi-exposed rocky shores. *Journal of Experimental Marine Biology and Ecology* **332**, 135–150.

Visscher PT, Stolz JF (2005) Microbial mats as bioreactors: populations, processes, and products. *Palaeogeography, Palaeoclimatology, Palaeoecology* **219**, 87–100.